JJEES

JJEES (2026) 17 (2): 266-276
ISSN 1995-6681

Jordan Journal of Earth and Environmental Sciences

Spatio-Temporal Dynamics of Land Surface Temperature and Urbanization Impacts in Bathinda City, Punjab (1990–2022)

Gurvinder Singh[1], Rohan Kumar[1], Jai Sukh Paul Singh[1], Swati Sharma[2*], Ajay Roy[1]

[1] Lovely Professional University, Phagwara, Punjab, India
[2] Center of Excellence, SEnSRS, Indian Institute of Technology (IIT), Ropar, Punjab, India

Received on 6 October 2025; Accepted on 12 January 2026

Abstract

This study examines the relationship between changing patterns of Land Surface Temperature (LST), land use/land cover (LULC) change, and vegetation index (NDVI) in Bathinda City, Punjab, India, over 32 years (1990–2022). Using the Landsat data, LST and NDVI were calculated for four years (1990, 1999, 2010, and 2022) and analyzed alongside the dynamics of LULC maps classification. Results show that the mean LST increased significantly from 31.2°C in 1990 to 36.6°C in 2022, indicating a rising urban heat island (UHI) effect. At the same time, vegetation cover declined sharply, with NDVI maximum values dropping from 0.71 to 0.46, while built-up and open lands expanded. Regression analysis confirmed a strong negative correlation between NDVI and LST, especially in 1990 (R^2 = 0.5604), but this relationship weakened in 2022 (R^2 = 0.1259), showing that vegetation alone can no longer explain urban heating. Spatial analysis shows that higher LST values are associated with urban and industrial zones, while cooler areas are linked to vegetation and water bodies. The findings highlight the impacts of rapid urbanization without sustainable planning as a major driver of LST rise in the study area. This study recommends integrating green infrastructure into urban development policies to reduce UHI effects.

Keywords: *Spatio-Temporal, LST, LULC, NDVI, UHI*

1. Introduction

Urbanization is now a strongly human-driven process that continuously alters the physical characteristics of the land surface and disrupts climate patterns in many parts of the world (Oke, 1982; Grimmond, 2007). As the cities are growing and with the increase of population, especially near the urban centers, ultimately the surrounding croplands and natural green areas are getting replaced by infrastructures such as roads, buildings, etc., which are inhibiting the natural capacity of a landmass to reflect the heat (Imhoff et al., 2010; Abusmier & Al-Kofahi, 2025). The increased absorption of natural light by built-up elements has increased the overall Land Surface Temperature (LST) in urban areas, which has led to the problem of Urban Heat Island (UHI) formation, making the urban centers hotter than the scattered settlements and vegetated areas (Voogt & Oke, 2003; Zhou et al., 2014). The UHI formation has caused many other issues, including increased power consumption, heatstroke among kids and the elderly, fire events in many urban areas due to overconsumption of cooling appliances, increased water consumption, and water scarcity in urban centers. (Santamouris, 2015; Li et al., 2019).

In India, the situation of urban expansion is critical, particularly in Tier II cities (Manesha et al., 2021), where the construction and development projects are not monitored as per standard building and environmental codes (Bhan & Jana, 2013; Tamrakar et al., 2024), ultimately leading to dense settlements with a more LST-elevating scenario. The added-on effects of soaring LST in cities are destroying natural vegetation, as plant water intake increases while resources are limited (Rao et al., 2021).

Bathinda, a fast-developing city located in the arid agro-climatic region of Punjab, is a very suitable example for studying LST dynamics over time and the resultant UHI effect. It is an important urban center, part of the Indo-Gangetic alluvial plains and has a semi-arid climate with large seasonal temperature ranges, thus sensitive to local environmental land-cover change, as well as anthropogenic heat sources (Majumder et al 2021). The establishment of major infrastructure, such as the Guru Nanak Dev Thermal Power Plant and an oil refinery, and associated industrial and residential growth has intensified built-up surfaces while reducing vegetation cover. Bathinda experienced substantial LULC transition in the form of growth in residential areas, commercial clusters, and industrial expansions. Studies based on geospatial technologies have noted an alarming decline in vegetation cover and an increase in settlement areas, culminating in a rise in localized surface temperature. ‘Bathinda’s climate is represented by extreme summer temperatures and low rainfall. When combined with rapid urban expansion, these climatic conditions contribute to increased thermal stress. This study offers insight into the thermal behavior of the land surface, which can be applied to other climatic zones in India.

Voogt and Oke (2003) studied the LST surface and atmospheric UHI mechanisms, heat reradiation, reflectance, and absorption from vegetated areas compared to the built-up area. Weng et al. (2004) mapped LST dynamics

* Corresponding author e-mail: swati.9238@gmail.com

by employing Landsat ETM+ imagery and LULC change analysis in Indianapolis. Similarly, Yuan and Bauer (2007) worked on high-resolution thermal data for change analysis in temperature patterns. Imhoff et al. (2010) studied the UHI effects across U.S. cities and confirmed its correlation with the increased LST after urban expansion activities. The UHI phenomenon in India has recently been a new hazard studied by many researchers: Kikon et al. (2016) applied the NDVI analysis to detect UHI formation in Guwahati, India; Pal and Ziaul (2017) studied spatio-temporal changes in LST in Kolkata using multi-year Landsat datasets; Sethi et al. (2024) combined NDVI and LST trends to analyze the impacts of urban sprawl in Bhubaneswar, India. Momeni and Saradjian (2007) and Bao et al. (2023) developed emissivity correction models using NDVI and LULC layers to enhance UHI analysis. Sobrino et al. (2004) and Jiménez-Muñoz et al. (2009) proposed a split-window algorithm for LST estimation in UHI analysis. Mallick et al. (2013) and Bao et al. (2023) used NDVI, Normalized Difference Built-up Index (NDBI), and Normalized Difference Water Index (NDWI) to examine LST dynamics and their correlation with heat gradients across varying LULC patterns. Rajasekar and Weng (2009) explored the role of bare soil and built-up areas in thermal amplification using ASTER imagery for Chennai. Tran et al. (2006) explored inter-city LST changes in relation to spatial variations in LULC layers. Buyantuyev and Wu (2010) reported urbanization patterns in Phoenix, USA that led to a lowering of groundwater levels and to evapotranspiration exceeding rainfall, thereby exaggerating the UHI impacts in the study area.

Despite this growing body of research, a critical gap remains. Most studies either lack temporal depth, analyzing only one or two years, or fail to integrate vegetation and moisture indices in a comprehensive way (Manjunath & Jagadeesh, 2024; Tamrakar and Sharma, 2024; Okoduwa & Amaechi, 2025). The methodological inconsistency across different sensors (Landsat, MODIS, ASTER) and the majority research interest in the Tier-1 cities like Delhi, Mumbai, Bangaluru makes long term analysis difficult, especially for cities located in arid and peri-urban regions of India like Bathinda city that requires a detailed LULC study for absolute calibrations of LST fluctuation, (Zhou et al., 2014; Li et al., 2019).

The primary objective of this study is to assess the spatio-temporal evolution of LST in Bathinda City from 1990 to 2022 using multi-temporal Landsat data. The LULC and vegetation indices, such as NDVI, were classified to evaluate their relationship with varying LST over the selected time period. Finally, the results estimate the intensity of the UHI effect and compare thermal differences between urban and peri-urban zones over the temporal timeline. Additionally, it seeks to identify the key LULC and biophysical factors influencing LST distribution through regression-based statistical modeling.

This study presents the first long-term (1990–2022) LST analysis for Bathinda City, Punjab, integrating environmental indices: NDVI-based emissivity and LULC patterns across multiple temporal timelines, and spectral indices for improved accuracy. Regression models are used to quantify LST–landscape relationships, offering data-driven insights. Overall, it offers a unique methodological and contextual contribution to urban remote sensing in arid Indian cities.

2. Study Area

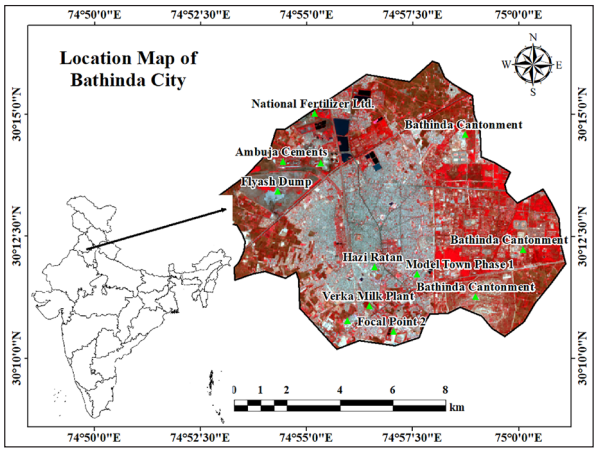

Figure 1. Map depicting the location of the study area, Bathinda City

Bathinda city is the oldest city of Punjab, situated between ”29º46’11” and ”30º35’08” north latitude and from ”74º37’49” and ”75º22’54” east longitude (Figure 1). It is located in the south-western part of Punjab and lies within the Indo-Gangetic alluvial plains. The region is mostly flat with gentle slopes, and the average elevation ranges from 200 to 220 meters above sea level. There are no hills or natural elevations; the landscape is mainly modified by human activities such as canals, embankments, and urban structures. The climate of Bathinda is semi-arid, characterized by very hot summers, mild winters, and low rainfall. In the summer months, especially May and June, the temperature often crosses 45°C, and hot winds called ‘’’loo’ are common in this region. Winters are cooler with minimum temperatures falling to 4–5°C. The annual average rainfall is about 400–500 mm (Sharma et al., 2017), which occurs mainly during the monsoon period from July to September, but the rainfall is often erratic and unevenly distributed. Soils in this region are sandy to sandy loam in texture, generally low in organic matter, and prone to salinity in some areas. Vegetation in Bathinda is mostly planted rather than natural, and trees are commonly found along roadsides, parks, and canals (Ahmad, 2023). The natural green cover is very sparse due to the dry climate. The main land-use pattern in and around Bathinda is agriculture, with wheat, cotton, and mustard as the dominant crops, supported by canal and tube-well irrigation. However, in recent years, the urban sprawl has converted agricultural lands into residential and commercial plots. Urbanization in Bathinda has picked up pace since the 1990s (Guite, 2019) due to industrial growth, improved transport connectivity, and the establishment of major public-sector units, such as thermal power plants and the Guru Gobind Singh Oil Refinery. This growth is mostly unplanned, with residential colonies and commercial buildings expanding on the periphery without proper infrastructure. The central areas are becoming overcrowded, and green spaces are

continuously shrinking, raising concerns for heat stress and environmental degradation. In the backdrop of impending climate change, where temperature extremes and weather unpredictability are expected to worsen, understanding urbanization patterns and their impacts on local land and climate systems becomes urgent. Bathinda, situated in a sensitive agro-climatic zone, needs immediate attention to climate-resilient urban planning, sustainable land use, and environmental monitoring to protect people and the ecosystem from rising heat and water-related stresses.

3. Materials and Methods

This study investigates the spatio-temporal evolution of LST and its role in UHI formation in Bathinda City, located in the south-western region of Punjab, India, over 32 years from 1990 to 2022. The research leverages geospatial techniques and satellite datasets to examine how thermal conditions have changed in Bathinda City, Punjab, due to rapid industrialization and urban growth.

The methodology involves processing multi-temporal satellite images, followed by LULC classification, NDVI variations in the study area based on analysis of thermal bands from Landsat sensors, and an urban–rural long-term temperature gradient estimate indicating UHI intensity. Further, multivariate statistical classification and modeling are used to identify key driving factors influencing LST patterns, including both natural and human-induced variables. The workflow is represented in Figure 2, providing a systematic overview of data input, processing, and analysis stages.

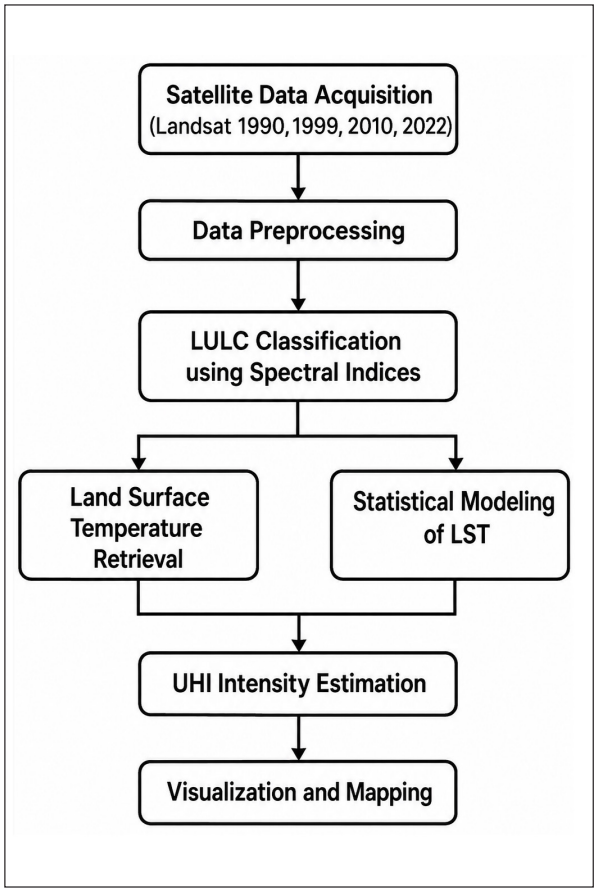

Figure 2. Diagram representing the overall methodology flowchart

Table 1. Details of Satellite Data Used in the Study

S.No	Satellite	Sensor	Year	Acquisition Date	Spatial Resolution	Bands Used	Cloud Cover	Season
1	Landsat 5	TM	1990	10 May 1990	30 m (optical & TIR)	Bands 1–7	<10%	Pre-monsoon
2	Landsat 5	TM	1999	15 May 1999	30 m (optical & TIR)	Bands 1–7	<10%	Pre-monsoon
3	Landsat 5	TM	2010	12 May 2010	30 m (optical & TIR)	Bands 1–7	<10%	Pre-monsoon
4	Landsat 8	OLI/TIRS	2022	08 May 2022	30 m (resampled TIR)	Bands 1–11	<10%	Pre-monsoon

3.1 Satellite data and pre-processing

In this study, multi-temporal satellite imageries were acquired from USGS Earth Explorer that included Landsat 5 TM bands for the years 1990, 1999, and 2010 and Landsat 8 OLI/TIRS for 2022 (Table 1). These data were selected for their temporal precision in the long-term analysis of the urban heat regime, and match the key stage of the urban change that happened in Bathinda City post the Indian financial reforms undertaken in 1991. Imagery was acquired from March to June (the pre-monsoon season in this region) to minimize vegetation masking and ensure seasonal surface temperature variation. The images acquired were Level-2 products; thus, no radiometric or atmospheric corrections were required. Individual band layers were stacked to generate single composite images for each scene, followed by assigning them UTM Zone 43N and WGS 84 projected coordinates. The projected images were then clipped to the area surrounding Bathinda City. All this was ensured by ensuring that each scene had <10% cloud cover and a pixel dimension of 30m x 30m. Open-source software, QGIS version 3.28, was used for pre-processing.

3.2 LULC classification using spectral indices

To accurately extract LULC classes from multi-temporal satellite images, a hybrid classification technique was adopted, which combines spectral index thresholding with supervised classification based on the Maximum Likelihood Classifier (MLC). This method helped better separate different land types, especially in a mixed, dry area like Bathinda. Five major LULC categories were defined for classification: built-up area, vegetation, agricultural land, open/barren land, and water bodies. To strengthen discrimination among these classes, a set of normalized spectral indices was computed from Landsat imagery reflectance bands. These included the NDVI, which is calculated as (NIR − RED) / (NIR + RED) and is effective for identifying vegetative cover; the NDBI, computed as (SWIR − NIR) / (SWIR + NIR), to highlight urban and constructed areas and the NDWI, calculated as (GREEN − NIR) / (GREEN + NIR), which helps in detecting water bodies. LULC classification was carried out using QGIS (version 3.28) with the Semi-Automatic Classification Plugin.

These spectral indices were utilized in combination

with original image bands to define clear, representative training samples for supervised classification. The classified outputs for each time period were subjected to accuracy assessment using the Kappa coefficient. Ground-truth points collected from field surveys and high-resolution Google Earth imagery were used for validation, particularly for the 2022 dataset, while historical images were used with visual interpretation for earlier years. This methodology ensured that the LULC maps generated were both consistent and reliable for temporal analysis.

3.3 LST retrieval from Landsat data

The single-channel algorithm (QGIS SCP plugin) was applied to estimate LST from thermal bands of Landsat 5 (Band 6) and Landsat 8 (Band 10). The process involved radiance calculation, conversion to brightness temperature, and surface emissivity correction using NDVI-derived emissivity models.

Radiance and Brightness Temperature Calculation

For Landsat 5 TM, radiance (L_λ) was calculated using:

$$L\lambda = \left(\frac{(L_{max} - L_{min})}{(QCAL_{max} - QCAL_{min})}\right) \times (QCAL - QCAL_{min}) + L_{min} \quad (1)$$

Where:

L_λ - Spectral radiance (W/m²·sr·µm)

QCAL - DN values

L_{max},L_{min} - Spectral radiance scaling constants from metadata

Brightness Temperature (BT) in Kelvin:

$$T_B = \frac{K_2}{ln\left(\frac{K_2}{L_\lambda} + 1\right)} \quad (2)$$

For Landsat 8 TIRS, top of atmospheric radiance (TOA) was calculated as:

$$L_\lambda = M_L \times Q_{cal} + A_L \quad (3)$$

BT from TOA radiance:

$$T_B = \frac{K_2}{ln\left(\frac{K_2}{L_\lambda} + 1\right)} - 273.15 \quad (4)$$

Where K_1, K_2, M_L and A_L are radiometric calibration constants available in the scene metadata (MTL file).

Surface Emissivity Estimation and LST Correction

To correct for surface emissivity (ε), the NDVI-based method was adopted. The proportion of vegetation (PV) was calculated as:

$$PV = \left[\frac{(NDVI - NDVI_{\min})}{(NDVI_{max} - NDVI_{\min})}\right]^2 \quad (5)$$

Surface emissivity (ε): =0.004×PV+0.986

Final LST in Kelvin:

$$LST = \frac{T_B}{1 + \left(\frac{\lambda . T_B}{\rho}\right) \ln(\varepsilon)} \quad (6)$$

Where:

λ =10.8µm (central wavelength for Band 10)

ρ = h × c/σ =1.438×10^{-2}m·K

h = 6.626×10^{-34}Js, c=2.998×10^8 m/s, σ =1.38×10^{-23} J/K

3.4 Urban Heat Island (UHI) Intensity Estimation

Urban heat island intensity was calculated using a binary zonal contrast method in QGIS software by delineating:

Urban core zones (high-density built-up areas)

Peripheral rural buffer zones (non-urban areas with vegetative/agricultural land)

$$UHI_{intensity} = LST_{urban} - LST_{rural} \quad (7)$$

4. Results and Discussion

4.1 Changes in Land Use and Land Cover (LULC)

Table 3. Land use land cover classes 1990, 1999, 2010 and 2022

Category Name	Area (Km²)	Area (Km²)	Area (Km²)	Area (Km²)
Agriculture	17.58	8.32	9.66	9.38
Built Up	17.79	23.99	26.56	28.86
Open Land	13.99	29.11	16.66	25.75
Vegetation	38.57	27.21	35.91	24.83
Water Body	2.07	1.37	1.21	1.18
Total	**90**	**90**	**90**	**90**

LULC maps for the years 1990, 1999, 2010 and 2022 were generated with overall accuracies of 83%, 85%, 89% and 82%, respectively. The Kappa values for these years were 0.79, 0.81, 0.86, and 0.77, respectively. The results of the LULC analysis reveal substantial change, as reflected in the generated LULC maps (Figures 3 & 4). Separately, spatial expansion maps were prepared as depicted in Figure 5. The proportions of the following 5 classes of LULC: vegetation, agricultural land, built-up area, open land and water bodies were found to be 43%, 20%, 20%, 15% and 2% respectively for the year 1990. LULC analysis of 1999 indicated a marked change: vegetation class decreased to 30%, agricultural land class decreased to 9%, built-up area increased to 26%, and open land class increased to 33%. It also indicated roughly no change in the area under the water body class. By 2010, the vegetation class again increased to 40%, the agriculture area class roughly remained the same at 11%, the built-up area further increased to 30%, the open land class at 18%, and the water body at 1%. Further analysis of the imagery from 2022 showed that vegetation dropped to 28%, the agriculture class remained stagnant at 10%, built-up area increased to 32%, open land increased to 29%, and waterbody remained at 1% (Table 2). LULC results for the period 1990-2022 clearly indicate that the built-up area, which was 17.79 km² in 1990,

increased to 28.86 km² in 2022. During the same period, open land increased by 84%. In contrast, there was a noticeable decline in natural and agricultural land cover: vegetation cover decreased by 36%, agricultural land decreased by 47%, and water bodies decreased by 43%. Figure 5 shows that in 1990, Bathinda City was limited to a 2 km circle; by 1999, it had started growing at the southeast and northwest flanks. But from 1999 onwards, the city limits have started growing in all direc.tTill till, 2010 it remained like, thatfrom but 2010 on,wards more foccity growth city was seethe west-southwest directiontions. Over the past 32 years, Bathinda city has changed a lot. Natural land is now less, and built-up and open land are more.

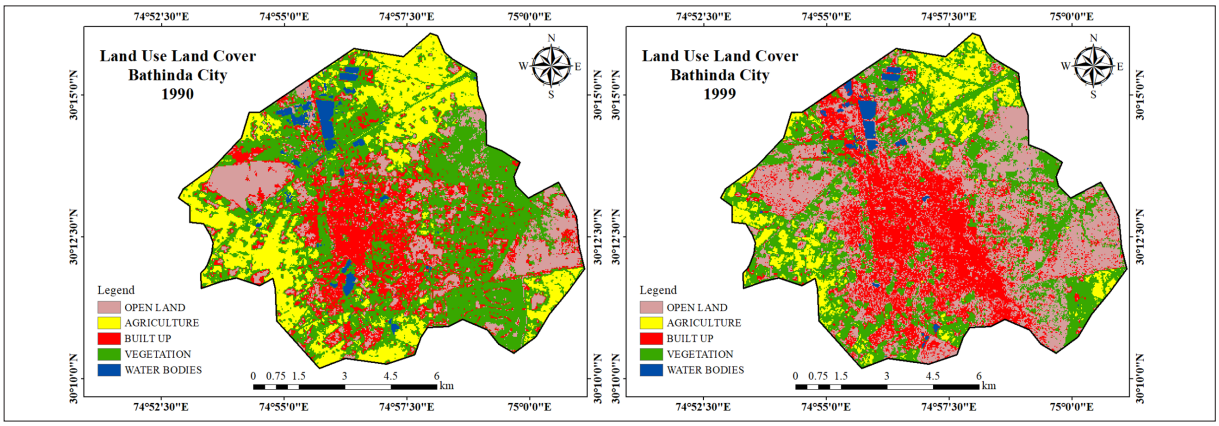

Figure 3. LULC classes of Bathinda city for the years 1990(left) and 1999 (right)

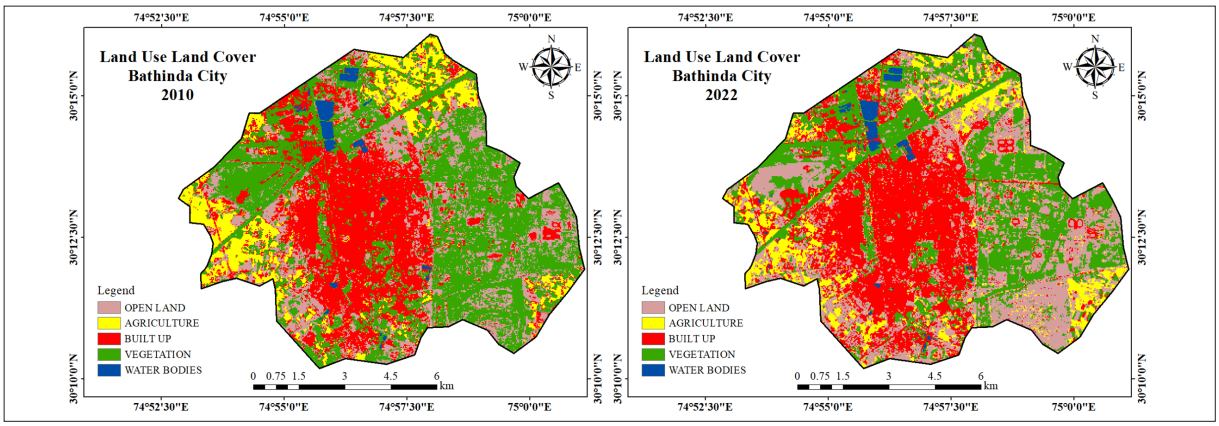

Figure 4. LULC classes of Bathinda city for the years 2010(left) and 2022 (right)

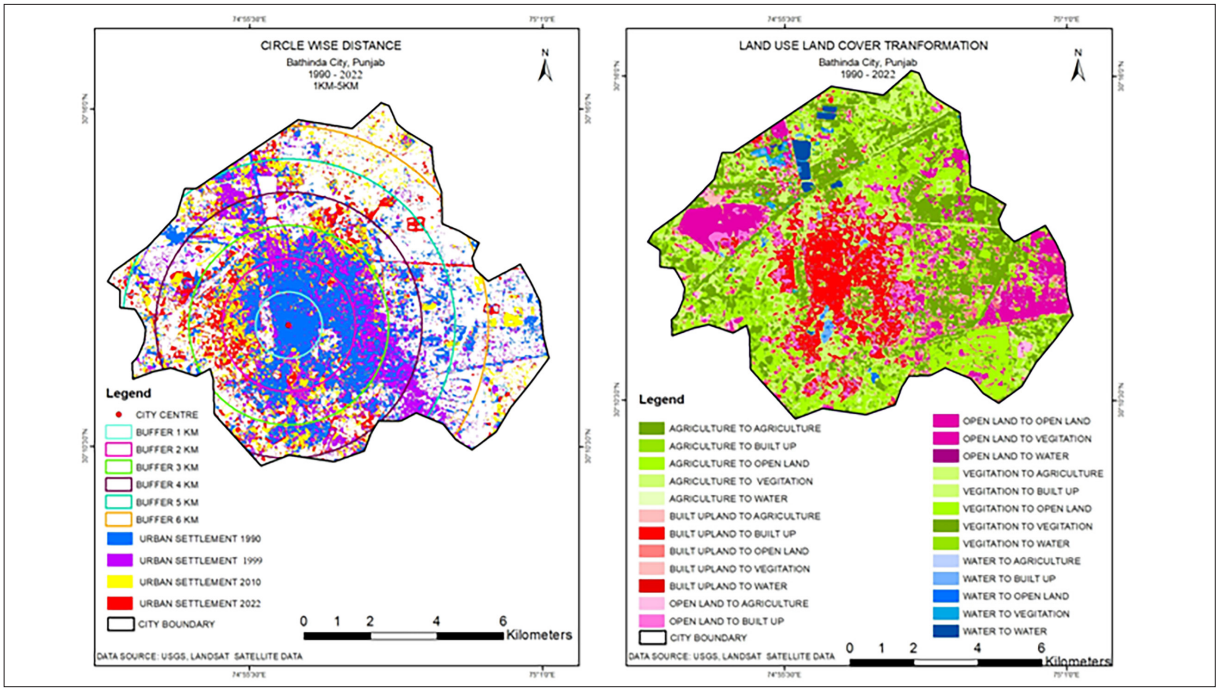

Figure 5. Spatial expansion from 1990 to 2022 (Left), Land Transformation from 1990 to 2022 (Right)

4.2. Land Surface Temperature (LST) Trends

The LST of Bathinda city has increased from 1990 to 2022. This change is clearly visible in the LST maps for the years 1990, 1999, 2010, and 2022 (Figures 6 & 7). In 1990, the average LST was about 31.2°C. By 2022, this increased to around 36.6°C. This shows that the city has become hotter over the last 32 years. The hottest areas were mostly in the city center and in industrial or built-up zones. These areas had more concrete and buildings, which absorb and trap heat. In contrast, the cooler areas were near vegetation, agricultural land, and water bodies. These natural surfaces help to keep the land cool by allowing evaporation and shading. The maps also show that the hot zones have spread outward from the center over time. In 1990, the high LST was mostly limited to the middle part of the city. By 2022, these hot areas had expanded in almost all directions, especially towards the west and southwest, where new development took place. This increase in temperature and the spreading of hot zones suggest a rise in the UHI effect, in which cities become hotter than surrounding rural areas due to buildings, roads, and less greenery. In summary, LST increased by more than 5°C between 1990 and 2022. Built-up areas are hotter, green/water areas are cooler, and hot zones now cover a larger part of the city, not just the center. Built-up areas are hotter, green/water areas are cooler, and hot zones now cover a larger part of the city, not just the center. These results show how urban growth and land changes have directly affected the temperature pattern in Bathinda.

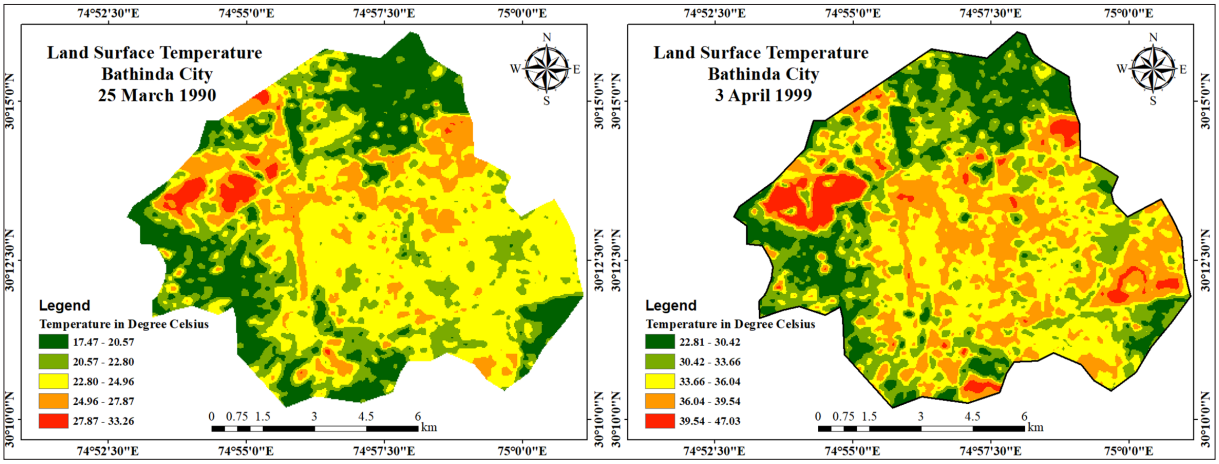

Figure 6. LST map derived from the Landsat sensor for the years 1990 (left) and 1999 (right) of Bathinda City

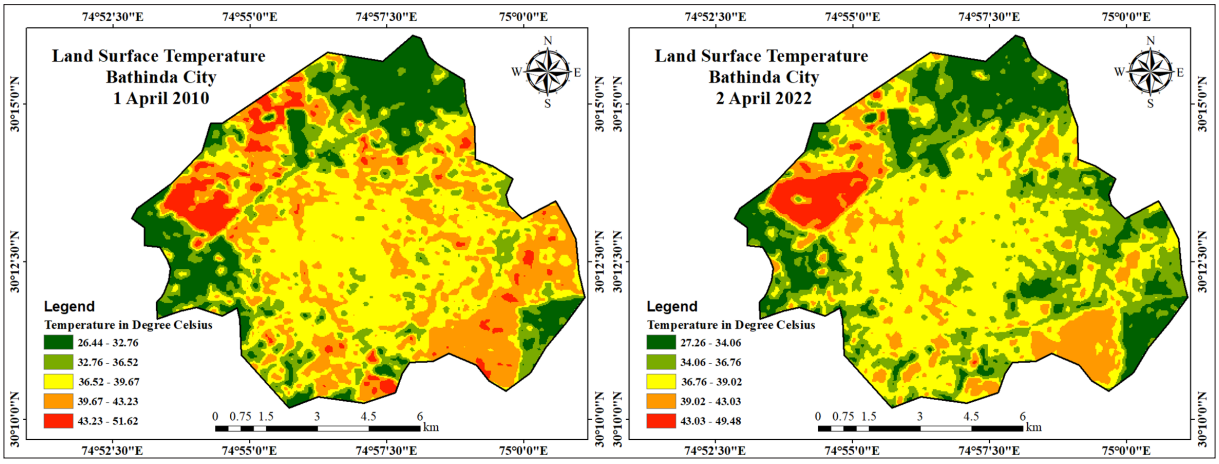

Figure 7. LST map derived from Landsat sensor for the year 2010 (left) and 2022 (right) of Bathinda City

4.3. NDVI Trends

The NDVI maps for 1990, 1999, 2010, and 2022 (Figures 8 & 9) show that green cover (vegetation) in Bathinda has decreased over time. In 1990, the maximum NDVI value was 0.71, indicating areas with dense green vegetation. The minimum NDVI value was –0.39, indicating the presence of non-vegetated areas, such as buildings, roads, or water. By 2022, the maximum NDVI had dropped to 0.46, and the minimum increased to –0.12. This difference means the greener areas became less green, and the non-vegetated areas increased. In 1990, more vegetation was observed in the northern and south-western parts of the city, as well as around the Cantonment area. Some green patches were visible in the center as parks. In 2022, these green zones had reduced in both size and health (lower NDVI values), and more areas showed lower NDVI values, indicating less or no vegetation. The central parts of the city and areas near industrial zones like the thermal power plant and National Fertilizer Limited (NFL) showed very low NDVI values in all years, especially in 2022, because of more buildings and very little greenery. The maps indicate that vegetation has decreased in both quantity and quality; NDVI values are declining each decade; and built-up and barren areas are increasing, while dense green areas are shrinking.

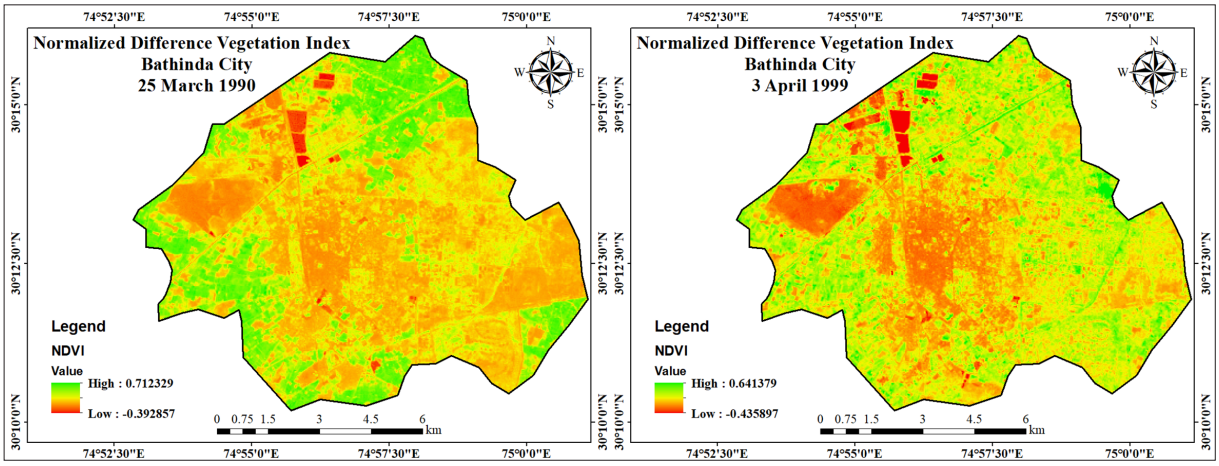

Figure 8. NDVI map derived from the Landsat sensor for the years 1990 (left) and 1999 (right) of Bathinda City

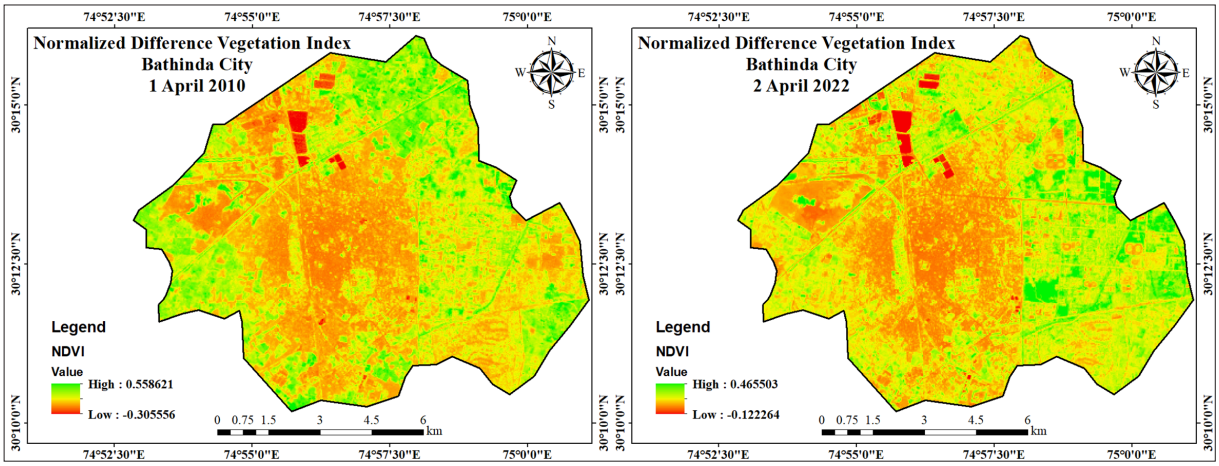

Figure 9. NDVI map derived from the Landsat sensor for the years 2010 (left) and 2022 (right) of Bathinda City

These results show that natural green cover is declining, which may lead to higher land surface temperatures and greater heat in the city, as discussed in the previous section.

4.4. Relationship between NDVI and LST

This section looks at how green cover (NDVI) and LST are related. We used scatter plots and regression analysis to study this for the years 1990, 1999, 2010, and 2022. The results are shown in Figures 10-13. In all four years, the relationship was negative, meaning that when NDVI is high (more vegetation), LST is low, and when NDVI is low (less vegetation), LST is high. The regression equations and R^2 values (which indicate the strength of the relationship) are shown in Table 3.

Table 3. Regression equations and R^2 values:

Year	Regression Equation	R^2 Value	Slope
1990	LST = 24.69 – 9.26 × NDVI	0.5604	–9.26
1999	LST = 36.35 – 12.24 × NDVI	0.1818	–12.24
2010	LST = 39.90 – 20.43 × NDVI	0.3251	–20.43
2022	LST = 39.26 – 13.31 × NDVI	0.1259	–13.31

From the Table, the strongest relationship was in 1990 (R^2 = 0.56). This result means NDVI explained 56% of the change in LST. In 2022, the relationship became much weaker (R^2 = 0.13). NDVI explained only 13% of the LST variation. This variation shows that in earlier years, green cover had a strong impact on land temperature. But over time, as the city developed and more concrete replaced greenery, other factors, (such as buildings, traffic, and roads) began to affect LST more than vegetation alone. The slope of the regression line was the steepest in 2010 (–20.43), indicating that a small change in vegetation caused a large change in temperature that year. This change might be due to rapid development and vegetation loss during that time. The effect of vegetation on LST was strong in the past, but weaker now due to more built-up land and other urban factors.

5. Discussion

5.1. Interpretation of LST and Urbanization Patterns

The LST maps for 1990, 1999, 2010, and 2022 (Figures 6 & 7) show that the temperature in Bathinda city has increased significantly over the last 32 years. In 1990, the average LST was about 31.2°C, but by 2022, it had reached about 36.6°C. This strong increase of more than 5 degrees Celsius shows a clear sign of the UHI effect. The hotter areas in the city are mostly where there is more built-up land and open land, especially in the city center and in industrial zones, such as near the Thermal Power Plant and the NFL area. These places have very little vegetation, so they absorb and keep more heat. The cooler areas are found near vegetated zones, agricultural fields, and water bodies. These natural surfaces help cool the land by releasing moisture and reflecting less heat. But over the years, these cooler areas have reduced in size. From the LULC maps (Figures 3 and 4), we can see that the built-up area increased from 20% in 1990 to 32%

in 2022. Vegetation decreased from 43% to 28%, and open land increased from 15% to 29%. This decrease means that natural land, such as trees and farms, is being replaced by concrete, roads, and bare land, which causes temperatures to rise. Also, urban expansion shifted from the city center to the northwest and southwest, especially from 1999 to 2022 (Figure 5). As the city grew, the hot zones also expanded, matching the direction of new construction.

The LST trend in Bathinda city closely relates to the city's progressive industrialization. In the early 1990s, a few agro-based units and thermal power infrastructure were in place, which evolved substantially over the years with the establishment of major energy and manufacturing facilities and planned industrial estates. Large industrial installations were commissioned in the 2000s, leading to the transformation of vegetated land to built-up land with high heat retention capacity. This study has clearly revealed thermal hotspots aligning with industrial corridors and urban zones. So, the rise in LST is closely connected with how the land is changing. More buildings and less green cover are making the city hotter. This is a serious issue for health, comfort, and the environment, and it shows that urban growth must be better planned to control rising temperatures.

5.2. NDVI decrease and green cover loss

The NDVI maps from the years 1990, 1999, 2010, and 2022 (Figures 8 & 9) show that green cover in Bathinda city has decreased a lot over time. In 1990, the maximum NDVI value was 0.71, but in 2022, it dropped to 0.46. This means there are fewer dense green areas now. The minimum NDVI value also changed: it was –0.39 in 1990 and became –0.12 in 2022. This shows that even the driest or most barren areas are becoming more common. In the NDVI map of 1990 the north, southwest, and cantonment area had high NDVI values. These were green and healthy zones. By 2022, many of these areas had turned into built-up or open land, and their NDVI values became low. The reason behind this drop in NDVI is seen in the land use change. This means green areas were either cut down for construction, turned into barren plots or used for roads and infrastructure. This change affects not only the look of the city, but also the environment. The NDVI maps clearly show this transformation and prove that green cover is shrinking fast in Bathinda. This also helps to explain why LST has increased, because less vegetation means more heat.

5.3. NDVI–LST relationship over time

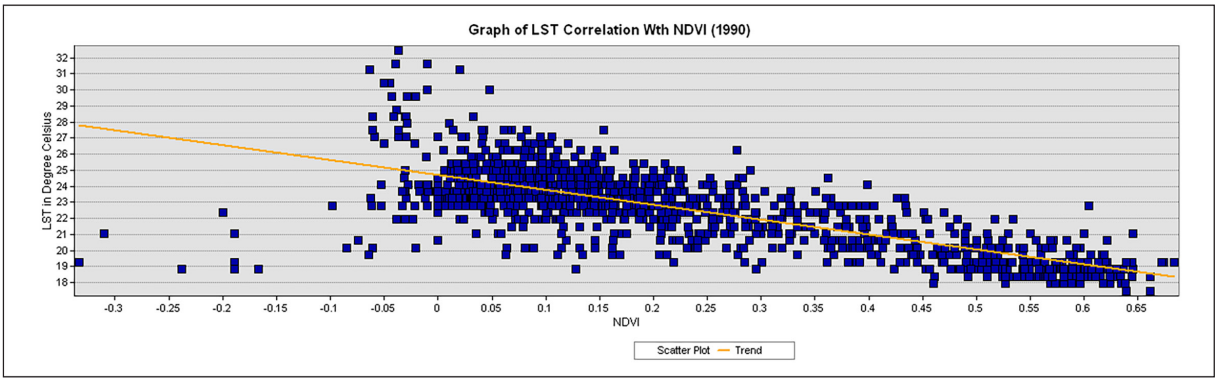

Figure 10. Scatter Diagram of 1990 showing the NDVI relationship with LST

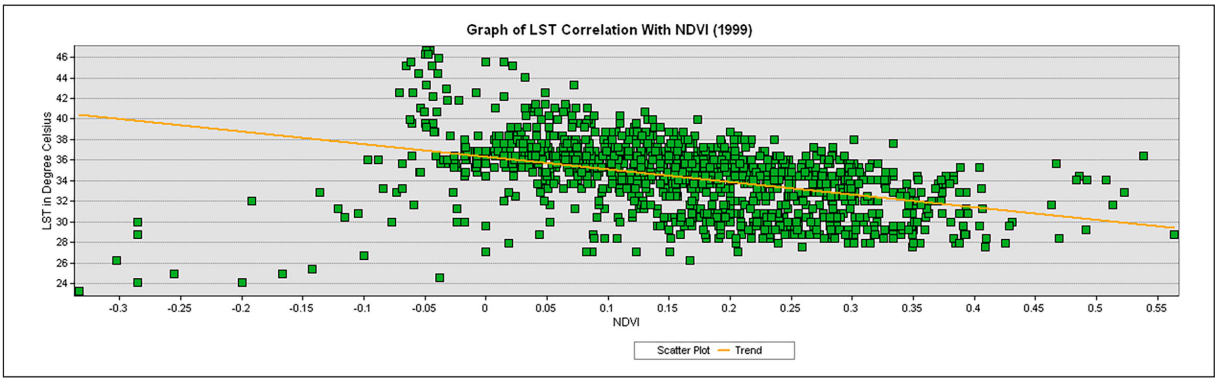

Figure 11. Scatter Diagram of 1999 showing the NDVI relationship with LST

The relationship between NDVI and LST was studied for 1990, 1999, 2010, and 2022 using scatter plots and regression analysis (Figures 10-13). In all four years, we found a negative relationship between NDVI and LST. This relationship means when NDVI is high, LST is low, and when NDVI is low, LST is high. This result is expected because vegetation helps to cool the land through evapotranspiration and shade. This change shows that NDVI and LST were strongly correlated in the past, but over time the relationship has weakened. 'That's because in 1990, the city had more vegetation and agriculture, so NDVI played a big role in cooling the surface. But in 2022, the city has more built-up areas, concrete roads, and industrial zones. These things also raise the temperature, but are not shown in NDVI. So now, LST depends on many urban factors, not just vegetation. NDVI alone cannot explain the high temperatures we see in today's urban landscape.

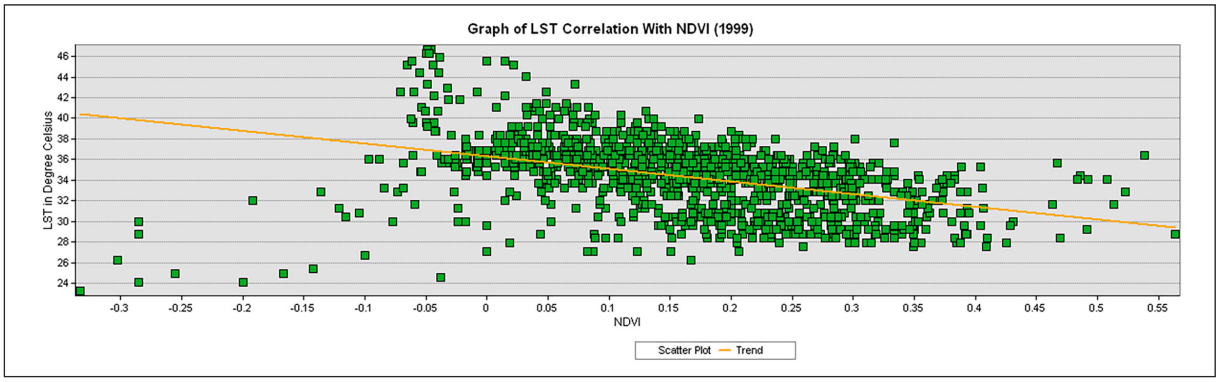

Figure 12. Scatter Diagram of 2010 showing the NDVI relationship with LST

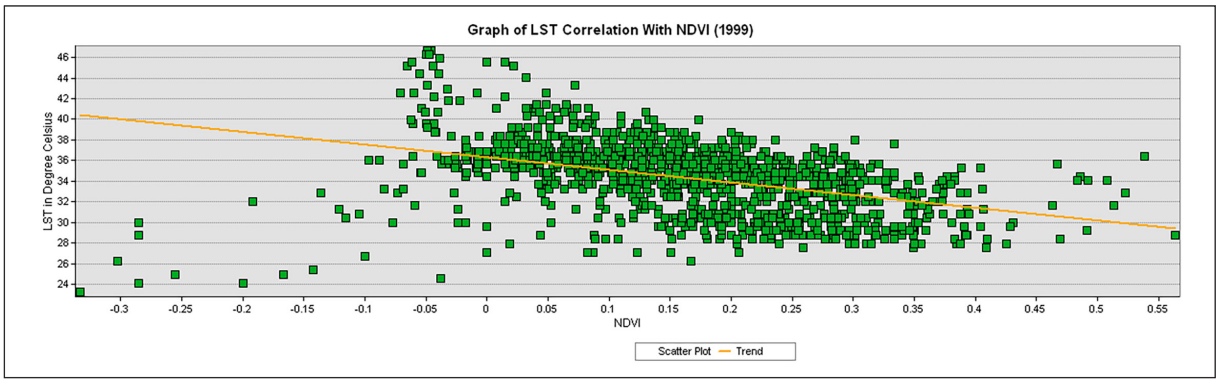

Figure 13. Scatter Diagram of 2022 showing the NDVI relationship with LST

The study clearly shows that urban growth in Bathinda has reduced green areas and increased LST. This is dangerous for the city's climate, health, and future development. The loss of vegetation and the rise in built-up and open land have intensified the urban heat island effect. If this continues, the city will face more heat stress, poor air quality, and health problems. To reduce these effects, urban planning should focus on saving and increasing green cover. This greening can be done by protecting parks, planting trees, and keeping green buffers around roads and buildings. Open land, which is rising in many parts, should not be left barren—it should be turned into green spaces or used wisely. New construction should include cool roofs, shaded areas, and less concrete. The city must also regularly monitor land use and temperature using satellite data , as done in this study. This strategy can help planners and government officials make smart decisions to manage heat and control unplanned expansion. Green and climate-friendly policies are now urgent, especially in rapidly growing cities like Bathinda.

6. Conclusion:

This study clearly shows that Bathinda city has become much hotter over the last 32 years due to urban growth and loss of vegetation. The Land Surface Temperature (LST) increased from 31.2°C in 1990 to 36.6°C in 2022, mainly in areas where built-up and open land have replaced green zones. The NDVI values dropped, showing a sharp decline in vegetation. The negative relationship between NDVI and LST shows that green cover helps reduce surface temperature. However, over time, this link weakened, indicating that vegetation alone cannot explain the city's temperature rise. The regression model errors increased, showing the limitation of using only NDVI to predict LST in urban areas. It is clear that other factors, such as buildings, roads, and land-use changes, also play a significant role in increasing temperatures. This study shows that remote sensing and satellite data are powerful tools to monitor land changes and support smart city planning. The results reflect the need to increase the urban vegetation, namely, parks, trees along the streets and green buffer zones that can reduce the thermal stress in dense urban pockets. Rejuvenation of barren land, former industrial land, etc., with green cover could further reduce local heat accumulation. Major causes of heat accumulation include unscientific roofing and impervious surfaces, which can be addressed through reflective roofing and reduced impervious surfaces in high-LST zones, lowering surface temperatures. These findings can assist town planners in the development of a sustainable urban environment.

Author Contribution

SN	Name of author	Contribution
1	Gurvinder Singh	Conceptualized this study. He collected satellite images, produced land-use and NDVI maps, and prepared the first draft of the report.
2	Dr. Rohan Kumar	Worked on the method to calculate LST and studied how LST changed over time.
3	Dr. Jai Sukh Paul Singh	Worked on a correlation study between NDVI and LST to improve the report with scientific inputs
4	*Dr. Swati Sharma	Worked on processing satellite data, creating maps, and preparing the final draft.
5	Ajay Roy	Helped in making clean and clear maps, organizing data, and finding related studies for background support.

Acknowledgment:

We would like to thank Lovely Professional University (LPU), Punjab, for its logistical and research support during this research. The university provided us with access to computers, software, the internet, and the library, which helped us accomplish this work.

Conflict of Interest:

The authors declare that there is no conflict of interest related to this study.

Funding Statement:

No funds were acquired for this work.

References

Ahmad, N. (2023). Spatio-Temporal Change Detection Analysis of Land Use Land Cover of Bathinda District, Punjab, India. Biosciences Biotechnology Research Asia, 20(2), 571-590.

Abusmier, S. A., & Al-Kofahi, S. D. (2025). Examining Land Use/Land Cover Dynamics in Zarqa Governorate Major Districts: Implications for Urban and Environmental Sustainability. Jordan Journal of Earth & Environmental Sciences, 16(1).

Okoduwa, A. K., Amaechi, C. F., & Enuneku, A. A. (2025). Assessing Land Use/Land Cover and Predicting Future Scenarios in Kano Metropolis, Northern Nigeria. Jordan Journal of Earth & Environmental Sciences, 16(3).

Bao, G., Qin, Z., Bao, Y., Zhou, Y., Li, W., & Sanjav, A. (2014). NDVI-based long-term vegetation dynamics and its response to climatic change in the Mongolian Plateau. Remote Sensing, 6(9), 8337-8358.

Bao, Y., Li, Y., Gu, J., Shen, C., Zhang, Y., Deng, X., & Ran, J. (2025). Urban heat island impacts on mental health in middle-aged and older adults. Environment International, 109470.

Bhan, G., Anand, G., Arakali, A., Deb, A., & Harish, S. (2013). Urban housing and exclusion. India exclusion report, 14, 77-108.

Buyantuyev, A., & Wu, J. (2010). Urban heat islands and landscape heterogeneity: linking spatiotemporal variations in surface temperatures to land-cover and socioeconomic patterns. Landscape ecology, 25, 17-33.

Chandra, S., Sharma, D., & Dubey, S. K., (2018). Linkage of urban expansion and land surface temperature using geospatial techniques for Jaipur City, India. Arabian Journal of Geosciences, 11, 1-12.

Grimmond, C. S. B. (2007). Urbanization and global environmental change: local effects of urban warming. The Geographical Journal, 173(1), 83–88.

Guite, L. S. (2019). Assessment of urban sprawl in Bathinda city, India. Journal of Urban Management, 8(2), 195-205.

Imhoff, M. L., Zhang, P., Wolfe, R. E., & Bounoua, L. (2010). Remote sensing of the urban heat island effect across biomes in the continental USA. Remote Sensing of Environment, 114(3), 504–513.

Jiménez-Muñoz, J. C., & Sobrino, J. A. (2009). Split-window coefficients for land surface temperature retrieval. International Journal of Remote Sensing, 30(8), 2147–2165.

Kaur, R., & Pandey, P. (2022). Spatial trends of surface urban heat island in Bathinda: a semiarid city of northwestern India. International Journal of Environmental Science and Technology, 1-22.

Kikon, N., Singh, P., Singh, S. K., & Vyas, A. (2016). Assessment of urban heat islands (UHI) of Noida City, India using multi-temporal satellite data. Sustainable Cities and Society, 22, 19–28.

Li, X., Zhou, Y., Asrar, G. R., Imhoff, M., & Li, X. (2019). Surface urban heat island response to urban expansion. Science of The Total Environment, 657, 710–720.

Majumder, A., Setia, R., Kingra, P. K., Singh, M., & Singh, S. (2021). Estimation of land surface temperature using different retrieval methods for studying the spatiotemporal variations of surface urban heat and cold islands in Indian Punjab. Environmental Development and Sustainability, 23, 15921–15942. https://doi.org/10.1007/s10668-021-01321-3

Mallick, J., Rahman, A., & Singh, C. K. (2013). Modeling urban heat islands in heterogeneous land surface and its correlation with impervious surface area by using night-time ASTER satellite data in highly urbanizing city, Delhi-India. Advances in Space Research, 52(4), 639-655.

Manesha, E. P. P., Jayasinghe, A., & Kalpana, H. N. (2021). Measuring urban sprawl of small and medium towns using GIS and remote sensing techniques: A case study of Sri Lanka. The Egyptian Journal of Remote Sensing and Space Science, 24(3), 1051-1060.

Manjunath, D. R., & Jagadeesh, P. (2024). Dynamics of urban development patterns on thermal distributions and their implications on water spread areas of Vellore, Tamil Nadu, India. Frontiers in Sustainable Cities, 6, 1462092.

Momeni, M., & Saradjian, M. R. (2007). Evaluating NDVI-based emissivities of MODIS bands 31 and 32 using emissivities derived by Day/Night LST algorithm. Remote Sensing of Environment, 106(2), 190-198.

Oke, T. R. (1982). The energetic basis of the urban heat island. Quarterly Journal of the Royal Meteorological Society, 108(455), 1–24.

Pal, S., & Ziaul, S. (2017). Detection of land use and land cover change and land surface temperature in English Bazar Municipality, India. The Egyptian Journal of Remote Sensing and Space Science, 20(1), 125–145.

Rao, Y., Dai, J., Dai, D., & He, Q. (2021). Effect of urban growth pattern on land surface temperature in China: A multi-scale landscape analysis of 338 cities. Land Use Policy, 103, 105314.

Santamouris, M. (2015). Regulating the damaged thermostat of the cities—Status, impacts and mitigation challenges. Energy and Buildings, 91, 43–56.

Sethi, S. S., Vinoj, V., Gogoi, P. P., Landu, K., Swain, D., & Mohanty, U. C. (2024). Spatio-temporal evolution of surface urban heat island over Bhubaneswar-Cuttack twin city: a rapidly growing tropical urban complex in Eastern India. Environment, Development and Sustainability, 26(6), 15381-15402.

Sharma, D. A., Rishi, M. S., Keesari, T., Pant, D., Singh, R., Thakur, N., & Sinha, U. K. (2017). Distribution of uranium in ground waters of Bathinda and Mansa districts of Punjab, India: inferences from an isotope hydrochemical study. Journal of Radioanalytical and Nuclear Chemistry, 313, 625-633.

Sobrino, J. A., Jiménez-Muñoz, J. C., & Paolini, L. (2004). Land surface temperature retrieval from LANDSAT TM 5. Remote Sensing of Environment, 90(4), 434–440.

Tamrakar, Y., & Sharma, S. (2024). A review of spatial analysis techniques used for LULC change detection over Delhi NCR in the past two decades. Geospatial technology to support communities and policy: pathways to resiliency, 263-287.

Tamrakar, Y., Das, I. C., & Sharma, S. (2024). Machine learning for improved drought forecasting in Chhattisgarh, India: a statistical evaluation. Discover Geoscience, 2(1), 84.

Tran, H., Uchihama, D., Ochi, S., & Yasuoka, Y. (2006). Assessment with satellite data for urban heat island in Asian mega cities. International Journal of Applied Earth Observation and Geoinformation, 8(1), 34–48.

Voogt, J. A., & Oke, T. R. (2003). Thermal remote sensing of urban climates. Remote Sensing of Environment, 86(3), 370–384.

Weng, Q., Lu, D., & Schubring, J. (2004). Estimation of land surface temperature–vegetation abundance relationship for urban heat island studies. Remote Sensing of Environment, 89(4), 467–483.

Yuan, F., & Bauer, M. E. (2007). Comparison of impervious surface area and normalized difference vegetation index as indicators of surface urban heat island effects. Remote Sensing of Environment, 106(3), 375–386.

Zhou, D., Zhao, S., Liu, S., Zhang, L., & Zhu, C. (2014). Surface urban heat island in China's 32 major cities: Spatial patterns and drivers. Remote Sensing of Environment, 152, 51–61.

Zhou, D., Zhao, S., Liu, S., Zhang, L., & Zhu, C. (2014). Surface urban heat island in China's 32 major cities. Remote Sensing of Environment, 152, 51–61.

Majumder, A., Setia, R., Kingra, P. K., Singh, M., & et al. (2021). Estimation of land surface temperature using different retrieval methods for studying the spatiotemporal variations of surface urban heat and cold islands in Indian Punjab. Environmental Development and Sustainability, 23, 15921–15942. https://doi.org/10.1007/s10668-021-01321-3